

High-Frequency Filters Manufactured Using Hybrid 3D Printing Method

Ubaldo Robles, Edgar Bustamante, Parya Darshni, and Raymond C. Rumpf*

Abstract—In this work, two different high-frequency filters were produced, and each was manufactured in two different ways, one using conventional PCB technology and the other using hybrid 3D printing. The hybrid 3D printing technique combined the use of microdispensing of conductive inks and fused filament fabrication (FFF) of thermoplastic substrates. Measurements, properties, and comparisons between these filters are discussed. The goal of the research was to benchmark 3D printing of high-frequency filters to more confidently manufacture sophisticated devices and high-frequency systems by hybrid 3D printing.

1. INTRODUCTION

3D Printing (3DP) holds great promise to revolutionize manufacturing. Over the last ten years, 3DP has progressed from a rapid prototyping tool to a true manufacturing technology capable of producing functional products [1]. In the electronics manufacturing industry, 3DP offers many opportunities, including the potential to develop 3D circuits that more effectively utilize the third dimension. The purpose of the present work is to compare simple microwave filters manufactured by conventional means to ones by 3DP. Some examples of 3D printed electronics include adding circuit elements to planar 3DP structures operating at 2.4 GHz [2], multi-layered electronics made by multi-material printers [4], efforts to find low cost materials to produce electronic sensors [3], 3DP of low frequency and direct current electronics [4], and the saving of weight and space by embedding electronics onto structures using 3D printing [1]. However, these efforts have not benchmarked the 3D printed high-frequency filters to their industry standard equivalents manufactured by conventional means.

In this effort, two simple filter designs were chosen that are mature and well understood in industry to make more meaningful comparisons. The devices were designed to filter signals around 2.4 GHz and compare performance differences between conventional printed circuit board (PCB) devices and hybrid 3DP devices. The conventional filters were manufactured as standard PCBs that utilized copper for the conductors and FR4 as the dielectric substrate. The hybrid 3DP filters had dispensed silver inks to form the conductors and acrylonitrile butadiene styrene (ABS) plastic as the dielectric substrate deposited via fused filament fabrication (FFF) [2]. Hybrid 3D printing was used to merge micro-dispensing and FFF into a single manufacturing process [5]. Using nScrypt hybrid 3D printing technology, we were able to handle 3D printed features, accuracy, and repeatability down to the micron size level [6]. Last, the devices were tested using an Agilent vector network analyzer (VNA), and the results compared show that this technology is able to form simple high-frequency circuits.

Mason and Sykes first introduced stepped impedance element filters in 1937 [8]. Then, the military desired this technology to be used in radar, band limiting, multiplexing, and electronic counter measures on their attempt to step up from the analogue lumped filters used at the beginning of WWII. The Radio Research Laboratory did much of the early work on band-pass distributed impedance filter to develop

Received 26 October 2018, Accepted 7 August 2019, Scheduled 27 August 2019

* Corresponding author: Raymond C. Rumpf (rcrumpf@utep.edu).

The authors are with the University of Texas at El Paso, USA.

coaxial filters for electronic countermeasure applications [7]. Telecommunication companies and other organizations with large data networks applied the microwave filters to their data broadcasting [8]. Nowadays, both technologies are found over most high frequency devices including satellite dish receivers, cellphones, as well as sensitive measuring equipment. From early on, the design of filters has been planar. With 3DP we can achieve smaller designs, arbitrary shapes, and save weight and space for filters that can be made more three dimensionally.

2. FILTER DESIGN DISCUSSION

Stepped and coupled-line impedance filters require no lumped elements, only two materials for manufacturing, and simple designs with breaks, stubs, holes, steps, and/or slits. These attributes make distributed element filters ideally suited to be 3D printed. Our two filter designs were: (1) a coupled-line bandpass filter, and (2) a stepped-impedance low pass filter. Both PCB and 3DP filter designs were based on microstrip transmission lines, but each was forced to use a different dielectric with a different permittivity. For this reason, the substrate thicknesses were adjusted in order to achieve comparable performance at 2.4 GHz. We found that the microstrip patterns themselves did not require adjustment, only the thickness of the substrates.

When simulating the PCB microwave filters, copper with a sheet resistivity of $\rho = 1.05 \text{ m}\Omega/\text{sq}$ was used for the microstrip line and ground plane [11]. The substrate was FR4-Epoxy material, which has a relative permittivity of 4.35 at 2.5 GHz with a loss tangent of 0.018 [10]. SMA connectors were installed on PCB filters using standard silver solder, while the microstrip and ground of the 3D printed filters used conductive silver epoxy with a resistivity of $\rho = 4 \times 10^{-6} \text{ m}\Omega/\text{sq}$ [12]. The microstrips were fabricated using DuPont's CB028 silver ink. This silver ink is mainly composed of nano and micro particle flakes that must come into intimate contact after curing in order to conduct. As a result, the resistivity of the silver ink ($\rho = 10 \text{ m}\Omega/\text{sq}$) is considerably higher than pure copper [13]. The relative permittivity of the ABS was measured using a Damaskos split-cavity resonator and VNA to be 2.5 with a loss tangent of 0.005. We used optical epoxy (EPO-TEK 353ND) to fix the standard SMA connectors on the plastic part of the substrates of the 3D printed filters to avoid connector breaks. In our simulations, wave ports were used to launch signals into the SMA connectors. Figure 1 shows the simulation model for the low pass filter. We included all the features needed to manufacture and measure our 3D printed and PCB filters into the simulation. We simulated S_{11} and S_{21} parameters using ANSYS[®] HFSS software, and we compared them to the measurement results, discussed later in the testing section.

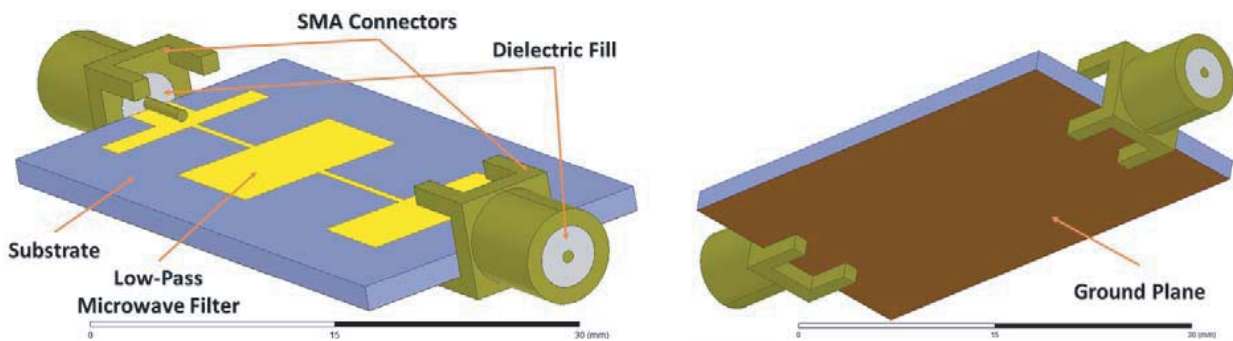


Figure 1. ANSYS simulation model for the low-pass filter.

2.1. Bandpass Filter

The coupled-line filter works by the frequency selectivity of directional coupling. We found though simulation sweeps that the impact of filter performance is negligible as long as the spacing between lines deviates by less than $10 \mu\text{m}$ [9]. Coupling was designed for microstrip lines separated by $432 \mu\text{m}$. Each line had a thickness of $25 \mu\text{m}$. The complete dimensions of the filter are shown in Figure 2. The filter was designed to operate at 2.4 GHz and provided a passband with fractional bandwidth of 10%.

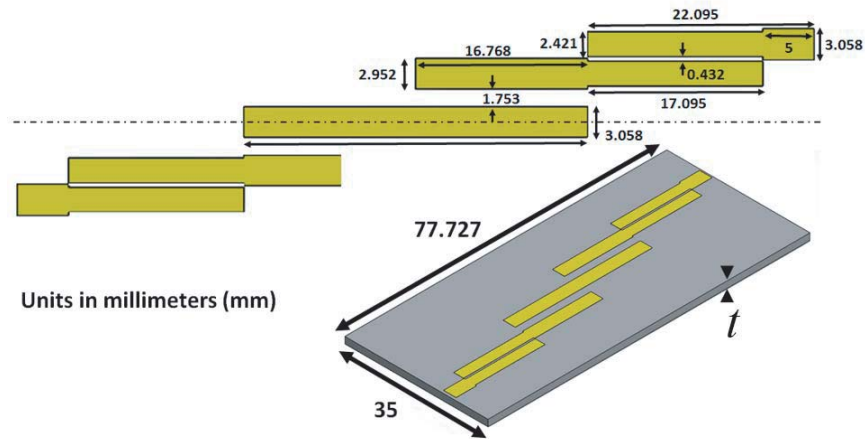


Figure 2. PCB design of the bandpass filter.

Thickness of the PCB substrate was 1.6 mm. SMA connectors were soldered onto the PCB boards using lead-free silver solder. The 3DP filter used silver ink as the conductor and ABS thermoplastic as the dielectric substrate. The ABS had a different dielectric constant from the FR4. In order to get equivalent performance with as few changes as possible, the substrate thickness of the 3DP device was made 1.54 mm to maintain consistent line impedance. The only dimensional difference between the PCB and 3DP designs was the thickness of the substrate.

2.2. Low Pass Filter

Next, we designed a simple low pass filter that attenuated signals above its cutoff frequency of 2.4 GHz [9]. Figure 3 shows the design of the low pass filter as well as its dimensions. The features in this filter were easier to manufacture by 3D printing because the geometry had no breaks and no closely spaced lines. Still, the 3DP challenge was to achieve similar dimension features that deviate less than

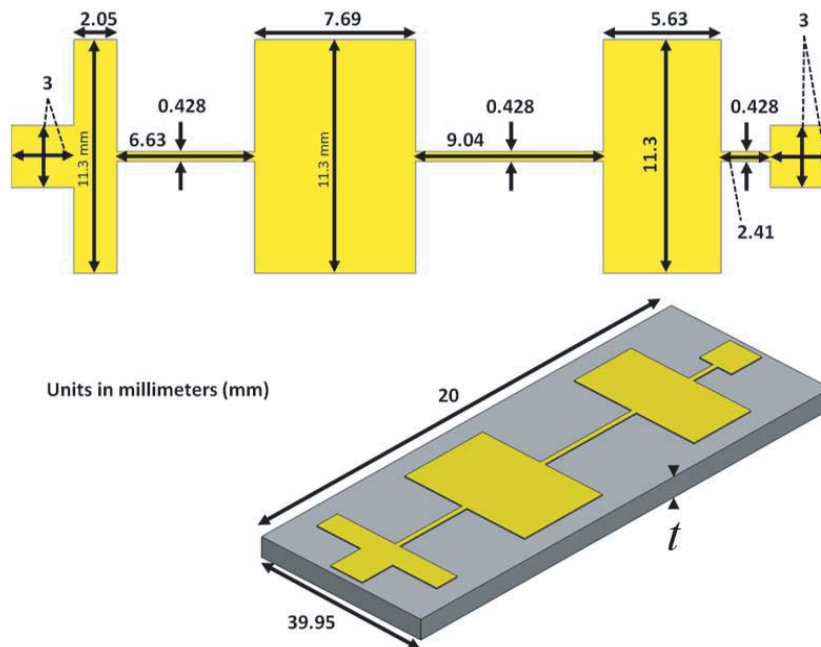


Figure 3. Filter design for the low pass filter.

10 μm as found in simulation sweeps for performance to be maintained. The same substrate thickness of 1.54 mm was used for the stepped-impedance filter. That was the only dimensional difference between the PCB and 3DP design.

3. MANUFACTURING

To manufacture the 3D printed versions of the filters, we used an nScript Tabletop series 3D printer, a hybrid 3D printer that is capable of depositing filaments via FFF and depositing pastes via microdispensing [2]. For microdispensing the silver conductive ink, we used nScript’s second-generation SmartPumpTM 100 system since it can control volume down to 100 pL, with a resolution of 0.1 μm , and produce metal lines as small as 12 μm in width and 10 μm in height by using nScript’s standard ceramic nTipsTM on their micro dispensing tool [14]. The desired width of the metal lines can be achieved by using the nTipsTM (900-4000-002) and adjusting the separation height between the printing surface and first layer dispensing height to 20 μm in width and 25 μm in height. The ABS dielectric was deposited using nScript’s nFDTM pump since it produced 120 μm line widths easily using nTipsTM (900-4000-002); it had a resolution of 0.1 μm [16]. In addition, there was a need to cure the silver ink with heat at 90°C using a heat blower [13].

Different software tools were used in order to process our design files for the 3D printed filters. First, Solidworks was used to design the geometry of the filters. We then divided the design into separate STL files for the dielectrics and conductors. These STL files for the dielectric portion were processed using Slic3r, a free software tool that generates g-code from the STL file to drive the 3D printer. Figure 4 shows the write path for 3DP. The STL file for the conductor portion was processed using an nScript proprietary software called PCAD that creates dispensing lines for the SmartPumpTM system. Last, both file processes are interpreted into a single g-code file by the nScript Tabletop printer. The g-code file controls the microdispensing and fuse deposition pumps of the printer creating our filters. Table 1 summarizes the optimized process parameters for producing high-quality devices.

There is a relation among ink viscosity, velocity of the pen tip, and dispense rate that affects the build [15]. We adjusted the speeds to dispense the material with as close to zero momentum as possible. These adjustments were necessary to avoid printing mistakes, gaps between printed lines on our surfaces, and more importantly created continuous layers that ink would leak through. It took 1 hour 28 minutes to build the low pass filter, and 3 hours 6 minutes to build the bandpass filter since it is twice as large as the low pass filter. Figure 5 shows the finished PCB and 3D printed filters.

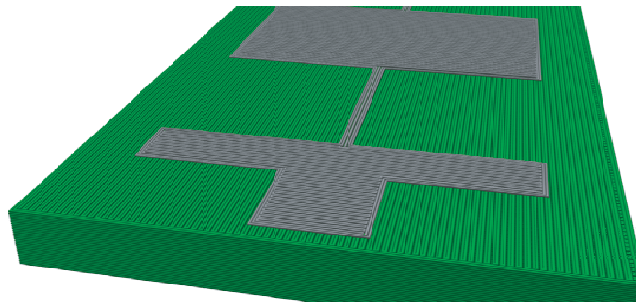


Figure 4. Tool path for 3D printed bandpass filter.

Table 1. Printing parameters.

Tool	nTips	Dispense gap	Print ratio	Print speed
SmartPump TM	100 μm	45 μm	1.06	60 mm/s
nFD TM	150 μm	110 μm	0.98	20 mm/s

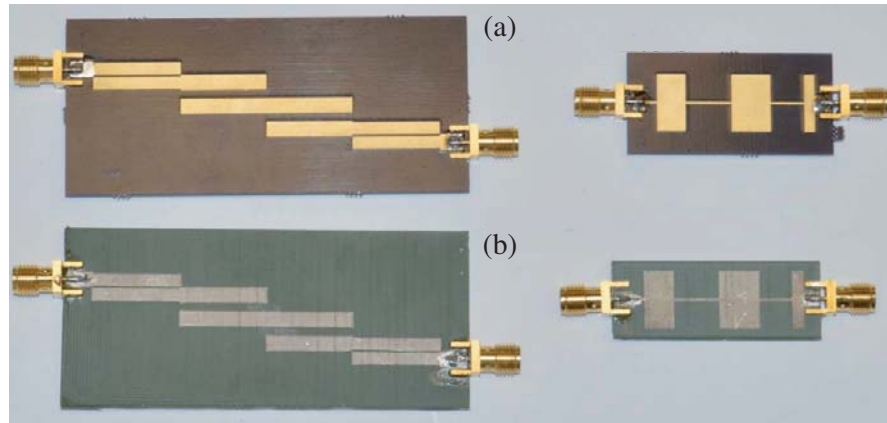


Figure 5. (a) PCB in contrast with (b) 3D printed filters.

4. TESTING

Overall, the test results show a slight frequency shift between the devices made by the two different manufacturing methods. An Agilent N5245A PNA-X vector network analyzer (VNA) with a 1601-point

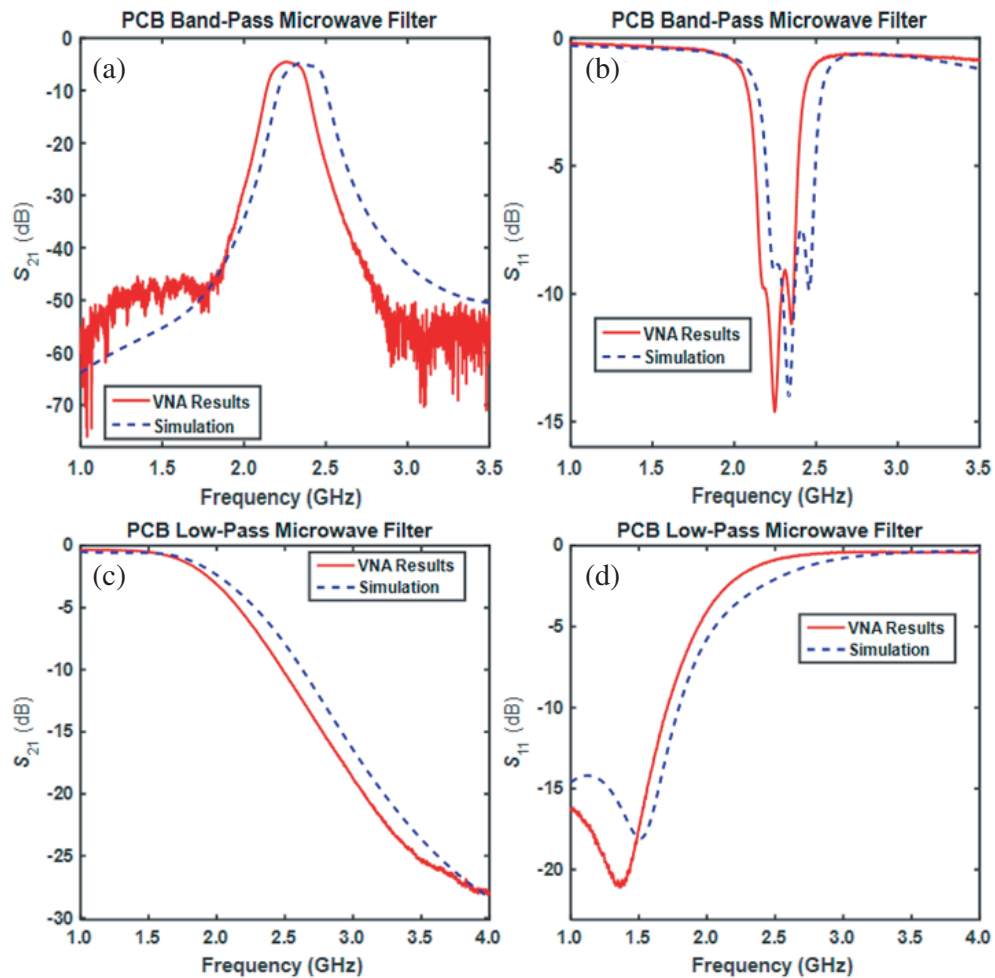


Figure 6. Results between manufactured PCB filters and their simulations.

sweep from 1 GHz to 4 GHz was used to measure all microwave filters. Figure 6 shows the measured S_{11} and S_{21} for the filter devices. All measurements in parts (a), (b), (c), and (d) indicate a small shift to lower frequencies compared to the simulated results due primarily to ohmic losses that were accounted for in the simulations. The SMA-microstrip transitions introduced some unintended reflections that produced standing waves, most obvious in the data for parts (a) and (b). Part (d) shows that the simulated S_{11} curve lies around 2 dB under the measured S_{11} , indicating higher reflections from the physical device than the simulated device. The most significant difference in transmission over all devices measured was 5 dB between the 3DP and simulated bandpass filters.

Figure 7 shows the measured S_{11} and S_{21} results for the 3DP filter devices. All measured devices show an expected response with a slight frequency shift, just like the results for the PCB filters [17]. The measured S_{21} in part (a) contains standing waves and noise before and after the target frequency due to the SMA-to-microstrip transition. Also, a slight frequency shift was observed that we attributed to surface roughness, lower conductivity on the microstrip by the use of silver ink over copper, and the decrease in effective dielectric constant between FR-4 and ABS plastic [19]. Part (b) shows a shift from 2.25 to 2.30 GHz due to the problems already identified. Part (c) shows the smallest frequency shift. Part (d) displays that the simulated S_{11} curve lies around 2 dB under the measured S_{11} , indicating higher reflections from the 3DP device. The results in this effort are constant with the shift in performance observed in a 3DP antenna array results tested at 2.45 GHz previously published by Ketterl et al. [2]. Part (d) in Figure 7 shows the measured filter exhibiting a 5 dB lower S_{11} than the simulated device, indicating that it outperformed our simulated device.

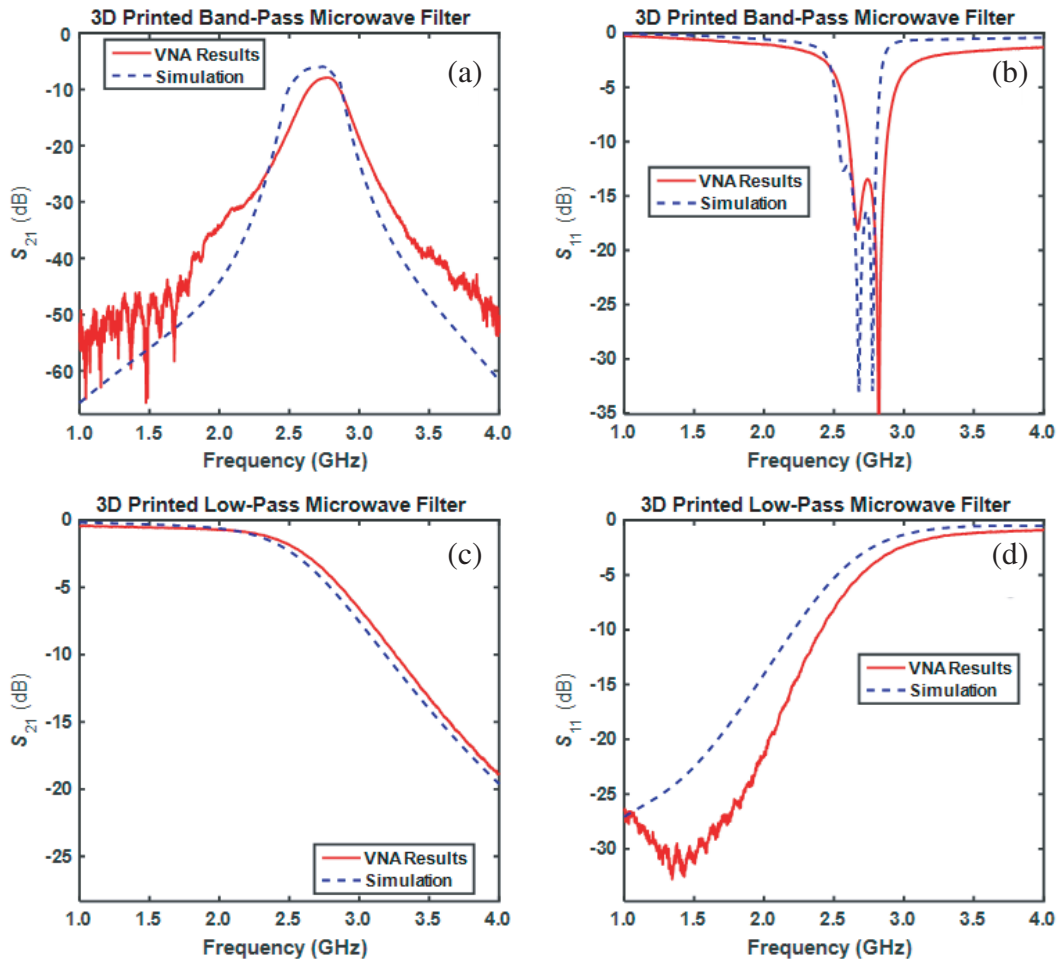


Figure 7. Results between 3D printed filters and their simulations.

5. DISCUSSION

Several factors contributed to the discrepancies between the performances of the PCB and 3DP filters. These factors include the conductivity of CB028 and the surface roughness of the 3D printed substrate. The temperature at which the silver paste is cured affects the conductivity of CB028 considerably. Thus, temperature needs to be controlled around the printing volume envelope to maintain precise control of conductivity. nFD produces relatively rough surfaces, and in combination with microdispensed conductive pastes creates a rough path for high frequency signals [2]. There is also a need for methodologies that adjust the printing process while printing since the inks can change consistency throughout the process [18]. We found that the lower permittivity of the ABS plastic led to designs utilizing a thinner substrate. Considering that 3D printing can produce structures with part air, we think 3DP can produce circuits that are smaller, lighter, and use less material to manufacture. This could have significant impact in volume manufacturing. We found it helpful to use thin paint films like polyurethane or epoxy to protect the printed conductors from oxidation. We also found it useful to incorporate features in the substrate that provide mechanical support for SMA connectors. There is a need to develop materials with lower loss, higher conductivity, and that are able to create smoother surfaces as they are 3D printed. Figure 8 summarizes the key differences between manufactured filters for this discussion.

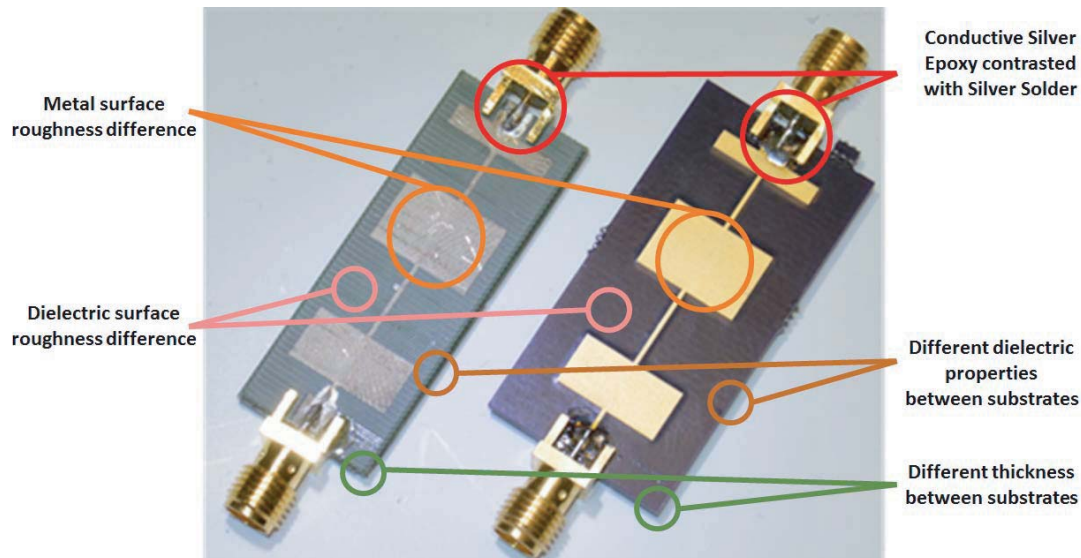


Figure 8. Points of comparisons between devices produced by different manufacturing processes.

6. CONCLUSION

The goal of this research was to compare hybrid 3D printed high-frequency devices to conventional PCB devices in order to test the feasibility of producing more complex devices and systems. To do this, we designed two simple RF filters and manufactured each using both standard PCB technology and 3DP. Our 3D printed devices were manufactured using a hybrid 3D printer from nScript that combined nScript's microdispensing of conductive inks and fused deposition of dielectric substrates.

When comparing the PCB device to the 3DP device, we observed only small differences in frequency of resonance, bandwidth of the response, and power loss. With further refinement in our 3D printing techniques, we conclude that direct-write 3D printing is a viable form of manufacturing for filter devices. Later on, we envision filters being more 3D, arbitrary, and saving space and weight [20].

ACKNOWLEDGMENT

This project was supported in part by U.S. Army Research Office (W911NF-13-1-01090). We would also like to acknowledge the expertise donated by nScript making this work possible.

REFERENCES

1. Gibson, I., D. W. Rosen, and B. Stucker, *Additive Manufacturing Technologies: Rapid Prototyping to Direct Digital Manufacturing*, Springer, 2010.
2. Ketterl, T. P., et al., "A 2.45 GHz phased array antenna unit cell fabricated using 3-D multi-layer direct digital manufacturing," *IEEE Transactions on Microwave Theory and Techniques*, Vol. 63, No. 12, 4382–4394, Dec. 2015, doi: 10.1109/TMTT.2015.2496180.
3. Leigh, S. J., R. J. Bradley, C. P. Purssell, D. R. Billson, and D. A. Hutchins, "A simple, low-cost conductive composite material for 3D printing of electronic sensors," *PLoS ONE*, Vol. 7, No. 11, e49365, 2012, doi: 10.1371/journal.pone.0049365.
4. Espalin, D., D. W. Muse, E. MacDonald, and R. B. Wicker, "3D printing multifunctionality: Structures with electronics," *The International Journal of Advanced Manufacturing Technology*, Vol. 72, No. 5, 963–978, May 2014.
5. Li, B., P. A. Clark, and K. H. Church, "Robust direct-write dispense tool and solutions for micro/meso-scale," *Proceedings of the 2007 International Manufacturing Science and Engineering Conference, MSEC 2007*, Atlanta, Georgia, USA, October 15–17, 2007.
6. Mohamed, O. A., S. H. Masood, and J. L. Bhowmik, "Optimization of fused deposition modeling process parameters: A review of current research and future prospects," *Advances in Manufacturing*, Vol. 3, No. 1, 42–53, March 2015.
7. Mason, W. P. and R. A. Sykes, "The use of coaxial and balanced transmission lines in filters and wide band transformers for high radio frequencies," *Bell Syst. Tech. J.*, Vol. 16, 275–302, 1937.
8. Levy, R. and S. B. Cohn, "A history of microwave filter research design and development," *IEEE Transactions on Microwave Theory and Techniques*, Vol. 32, No. 9, 1055–1067, 1984, ISSN 0018-9480.
9. Pozar, D. M., *Microwave Engineering*, John Wiley & Sons, 2009.
10. Aguilar, J. R., M. Beadle, P. T. Thompson, and M. W. Shelley, "The microwave and RF characteristics of FR4 substrates," *IEE Colloquium on Low Cost Antenna Technology*, (Ref. No. 1998/206), 2/1–2/6, London, 1998.
11. National Bureau of Standards, *Circular of the Bureau of Standards: Vol. 31, Copper Wire Tables*, No. 31, 71, MARCXML Washington Govt. Print, 1914.
12. Sarvar, F., N. J. Poole, and P. A. Witting, "PCB glass-fibre laminates: Thermal conductivity measurements and their effect on simulation," *Journal of Electronic Materials*, Vol. 19, No. 12, 1345–1350, December 1990, doi:10.1007/BF02662823.
13. Technical Data Sheet, "DuPont CB028 Silver Conductor," Vol. 19, 1345, doi: 10.1007/BF02662823, [online] <http://www.mcm.dupont.com>.
14. nScript Specification Sheet, "SmartPump™ 100 Specification Sheet," nScript Inc. Orlando, FL, [Online] <https://www.nscript.com> [<https://www.nscript.com/wp-content/uploads/2018/11/nScript-SmartPump-Gen2-2018.pdf>].
15. Vaezi, M., H. Seitz, and S. Yang, "A review on 3D micro-additive manufacturing technologies," *Int. J. Adv. Manuf. Technol.*, Vol. 67, 1721–1754, Springer-Verlag, London, 2012, doi 10.1007/s00170-012-4605-2#.
16. nScript Specification Sheet, "nFD™ Specification Sheet," nScript Inc. Orlando, FL, [online] <http://www.nscript.com> [<http://webolistic.com/nscript-624/wp-content/uploads/2018/08/nScript-SmartPump-Gen2-2018.pdf>].
17. Luukkonen, O., S. I. Maslovski, and S. A. Tretyakov, "A stepwise Nicolson-Ross-Weir-based material parameter extraction method," *IEEE Antennas and Wireless Propagation Letters*, Vol. 10, 1295–1298, 2011.

18. Church, K., E. MacDonald, P. Clark, R. Taylor, D. Paul, K. Stone, M. Wilhelm, F. Medina, J. Lyke, and R. Wicker, "Printed electronic processes for flexible hybrid circuits and antennas," *Flexible Electronics & Displays Conference and Exhibition, 2009*, 1–7, February 2–5, 2009.
19. Nam-Soo, K. and H. N. Kenneth, "Future direction of direct writing," *J. Appl. Phys.*, Vol. 108, 102801, [online], available: <http://dx.doi.org/10.1063/1.3510359>, November 2010.
20. Carranza, G., U. Robles, C. L. Valle, J. J. Gutierrez, and R. C. Rumpf, "Design and hybrid additive manufacturing of 3D/volumetric electrical circuits," *IEEE Trans. on Components, Packaging, and Manufacturing Technology*, 2019.